The microtubule poison vinorelbine kills cells independently of mitotic arrest and targets cells lacking the APC tumour suppressor more effectively

Daniel M. Klotz[1], Scott A. Nelson[1], Karin Kroboth[2], Ian P. Newton[1], Sorina Radulescu[3], Rachel A. Ridgway[3], Owen J. Sansom[3], Paul L. Appleton[1] and Inke S. Näthke[1,*]

[1]Division of Cell and Developmental Biology, [2]Division of Molecular Medicine, University of Dundee, Dow Street, Dundee, DD1 5EH, UK
[3]The Beatson Institute for Cancer Research, Garscube Estate, Switchback Road, Bearsden, Glasgow, G61 1BD, UK
*Author for correspondence (i.s.nathke@dundee.ac.uk)

Accepted 28 September 2011
Journal of Cell Science 125, 887–895

doi: 10.1242/jcs.091843

Summary

Colorectal cancers commonly carry truncation mutations in the adenomatous polyposis coli (*APC*) gene. The APC protein contributes to the stabilization of microtubules. Consistently, microtubules in cells lacking APC depolymerize more readily in response to microtubule-destabilizing drugs. This raises the possibility that such agents are suitable for treatment of APC-deficient cancers. However, APC-deficient cells have a compromised spindle assembly checkpoint, which renders them less sensitive to killing by microtubule poisons whose toxicity relies on the induction of prolonged mitotic arrest. Here, we describe the novel discovery that the clinically used microtubule-depolymerizing drug vinorelbine (Navelbine) kills APC-deficient cells in culture and in intestinal tissue more effectively than it kills wild-type cells. This is due to the ability of vinorelbine to kill cells in interphase independently of mitotic arrest. Consistent with a role for p53 in cell death in interphase, depletion of p53 renders cells less sensitive to vinorelbine, but only in the presence of wild-type APC. The pro-apoptotic protein BIM (also known as BCL2L11) is recruited to mitochondria in response to vinorelbine, where it can inhibit the anti-apoptotic protein BCL2, suggesting that BIM mediates vinorelbine-induced cell death. This recruitment of BIM is enhanced in cells lacking APC. Consistently, BIM depletion dampens the selective effect of vinorelbine on these cells. Our findings reveal that vinorelbine is a potential therapeutic agent for colorectal cancer, but they also illustrate the importance of the APC tumour suppressor status when predicting therapeutic efficacy.

Key words: Adenomatous polyposis coli, Apoptosis, Vinorelbine, Microtubules, BIM

Introduction

Colorectal cancers commonly carry truncation mutations in the adenomatous polyposis coli gene. APC protein plays a role in microtubule stability, and loss of APC directly decreases microtubule stability. This change is at least partly responsible for the mitotic and apoptotic defects in APC-deficient cells (Dikovskaya et al., 2007; Fodde et al., 2001; Kita et al., 2006; Kroboth et al., 2007). Nevertheless, APC deficiency does not render cells more sensitive to death induced by the microtubule poisons taxol and nocodazole, largely because these cells have a partially compromised mitotic checkpoint (Dikovskaya et al., 2007). To determine whether the increased sensitivity of microtubules in APC-deficient cells could be exploited nevertheless, we further explored the effect of microtubule poisons on cells and tissue with different APC status.

Microtubule poisons are commonly used as therapeutic agents for cancer (Ellis et al., 1999). Their mode of action relies on changing microtubule dynamics, which disrupts formation of mitotic spindles. Taxol stabilizes microtubules and prevents microtubule depolymerization, whereas nocodazole and vinca alkaloids, such as vinorelbine, prevent polymerization (Beswick et al., 2006; Verdier-Pinard et al., 1999). In each case, loss of dynamic instability results in lack of normal microtubule function, which can lead to cell death following prolonged mitotic arrest (Gascoigne and Taylor, 2008; Varetti and Musacchio, 2008). Therefore, these drugs kill highly proliferative cancerous cells (Jordan and Wilson, 2004). However, this might only partially explain the therapeutic effect of these agents (Letai, 2008).

Although both nocodazole and vinorelbine lead to loss of polymerized microtubules, their modes of action, efficacy and toxicity differ (Perez, 2009; Uppal et al., 2007). Nocodazole induces mitotic arrest by activating the spindle assembly checkpoint (SAC) (Beswick et al., 2006; Varetti and Musacchio, 2008). Given that nocodazole impairs microtubule–kinetochore attachment, cells arrest in metaphase owing to an active SAC. Most commonly, cell death follows prolonged mitosis (Gascoigne and Taylor, 2008; Huang et al., 2009) but premature mitotic exit into tetraploid G1 can occur as a result of inappropriately decreased cyclin B1 levels, even in the presence of an active SAC. Vinorelbine was thought to act similarly to nocodazole by arresting cells in mitosis (Gonzalez-Cid et al., 1997). Although both drugs cause depolymerization of microtubules, vinorelbine induces the formation of tubulin paracrystals (Jean-Decoster et al., 1999), and might also downregulate the anti-apoptotic protein BCL2 in a p53-dependent manner (Bourgarel-Rey et al., 2009). These effects might explain the efficacy of vinorelbine as a chemotherapeutic agent in some cancers (Conroy, 2002).

Journal of Cell Science

Colorectal cancers commonly carry truncation mutations in the *APC* gene (Kinzler et al., 1991). The connection between APC, colorectal cancers and microtubules, together with the paucity of chemotherapy available for this disease prompted us to explore the mechanisms of vinorelbine-induced cell death (Zumbrunn et al., 2001). Loss of APC directly decreases microtubule stability and this change is at least partly responsible for the mitotic defects in APC-deficient cells (Dikovskaya et al., 2007; Fodde et al., 2001; Kita et al., 2006; Kroboth et al., 2007).

We found that vinorelbine, unlike nocodazole, induces significant cell death during interphase, suggesting that its activity is independent of prolonged mitotic arrest. Consistent with this finding, vinorelbine-induced apoptosis was lower in cells depleted of p53. Importantly, vinorelbine-induced apoptosis was higher in APC-depleted cells, even in cells lacking p53. Cell death induced by vinorelbine was accompanied by an increase in BIM (also known as BCL2L11) protein at mitochondria. BIM inhibits BCL2, so the recruitment of BIM to mitochondria correlates well with the increased apoptosis induced by vinorelbine in APC-deficient cells. This might also explain how vinorelbine induces cell death during interphase without mitotic arrest (Puthalakath et al., 1999). Consistent with the idea that enhanced recruitment of BIM is involved in the sensitivity of APC-deficient cells to vinorelbine, depletion of BIM decreased the sensitivity of APC-deficient cells.

These findings suggest that vinorelbine could be a useful chemotherapeutic agent for the treatment of colorectal cancer.

Results

Vinorelbine induces cell death in interphase and targets cells lacking APC more effectively

The extremely common lack of fully functional APC in colorectal cancers makes it attractive to exploit selective defects of such cells for therapy. Unlike the tumour suppressor p53, which contributes to apoptosis during interphase and in response to prolonged activation of the SAC (Castedo et al., 2004; Chi et al., 2009), APC has only been shown to contribute to the latter, and cells depleted of APC are more resistant to apoptosis induced by prolonged SAC activation (Chen et al., 2003; Dikovskaya et al., 2007). To explore further the contribution of APC status to cell killing by microtubule poisons, we tested how APC-deficient cells responded to vinorelbine in therapeutically relevant doses (Degardin et al., 1994) (Fig. 1A). We found that cell death induced by vinorelbine was more pronounced in cells lacking APC, indicated by the increased number of cells containing active caspase-3 (aCasp3) after 4 hours of vinorelbine treatment at a range of concentrations (Fig. 1A). This rapid response to vinrorelbine suggested that death did not involve mitotic arrest.

Microtubule poisons are generally thought to kill cells as a result of prolonged mitotic arrest (Jordan and Kamath, 2007);

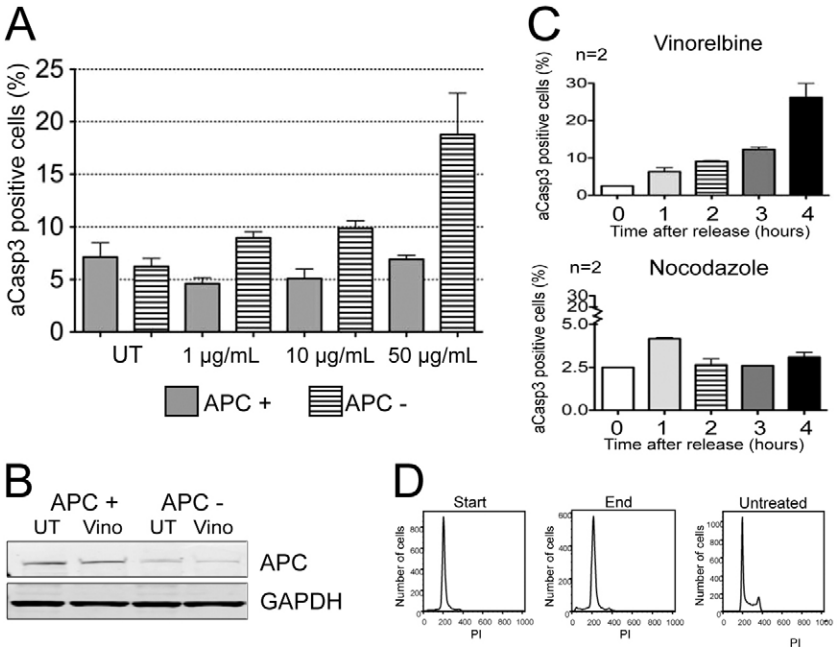

Fig. 1. APC deficiency increases vinorelbine-induced cell death. (**A**) Control (APC +) or APC-depleted (APC -) U2OS cells were exposed to the indicated concentrations of vinorelbine for 4 hours, fixed with PFA, stained for aCasp3 and analyzed using flow cytometry. Cells from ten independent samples were harvested for control cells and six independent samples for cells treated with vinorelbine. For each sample 10,000 cells were analyzed in each case. Results are means±s.e.m. UT, untreated. (**B**) APC depletion in control (UT) and vinorelbine-treated (Vino) U2OS cells. Immunoblots show successful depletion of APC with GAPDH as the loading control. Cells were treated with scrambled (APC +) or APC-targeting (APC -) siRNA and total lysates prepared from untreated control (UT) or vinorelbine-treated (100 µg/ml, 4 hours) cells. (**C**) Vinorelbine induces cell death during interphase, whereas nocodazole does not. U2OS cells were arrested in S phase using thymidine as described previously (Dikovskaya et al., 2007). Cells were then treated with either 50 µg/ml vinorelbine or 0.2 µg/ml nocodazole for the indicated times and the number of aCasp3-positive cells was measured by flow cytometry. Vinorelbine induced cell death in G1-arrested cells, whereas nocodazole did not. (**D**) U2OS cells do not enter G2 or mitosis 4 hours after release from thymidine. Control cells and thymidine-arrested cells were collected 0 hours (Start) and 4 hours after (End) thymidine release and fixed with ice-cold ethanol, and stained with PI for measuring of DNA content using flow cytometry. Cells did not enter G2 during this time window as indicated by the lack of a 4N DNA peak. The same profiles were obtained in cells treated with vinorelbine or nocodazole after thymidine arrest.

however, APC-deficiency has previously been show to protect against this process (Dikovskaya et al., 2007). To determine whether vinorelbine induces cell death during interphase or mitosis, we arrested cells in G1 with thymidine and treated them with vinorelbine or nocodazole (Fig. 1C,D). We measured aCasp3 every hour for 4 hours. After 4 hours, 26% of cells treated with vinorelbine were aCasp3 positive, whereas nocodazole treatment caused no change in the percentage of aCasp3-positive cells (Fig. 1C). Cells did not enter mitosis during this short experiment, as indicated by the lack of cells with 4N DNA content (Fig. 1D). This suggested that vinorelbine, but not nocodazole, induces apoptosis during interphase in G1.

We used RNA interference (RNAi) to deplete APC and p53 and routinely achieved 80–90% reduction in protein levels as shown by immunoblotting (Fig. 1B, 3A, 4A). Similar depletion was achieved in all subsequent experiments.

Vinorelbine induces cell death independently of cell cycle stage

The experiments described above only revealed snapshots in time of cell populations (Fig. 1) and could not completely differentiate between cells dying during mitosis or cells dying after a failed mitosis, such as those resulting in tetraploidy or aneuploidy (Dikovskaya et al., 2007). To determine more precisely at what point during the cell cycle cells in an asynchronous population died when treated with vinorelbine, we monitored cells using time-lapse movies (Fig. 2; supplementary material Fig. S1B,C). To identify apoptotic cells, we used Nucview, a fluorescent reporter for active caspase-3 (Cen et al., 2008). In parallel, we used mCherry-labeled lamin B1 to report on the integrity of the nuclear envelope as a marker for interphase cells (Liu et al., 2003). Given that p53 is an important player in inducing apoptosis and is commonly mutated in many cancers, including colorectal cancer, we also compared the contribution of p53 to these responses by depleting p53 with small interfering RNA (siRNA). First, we measured the cell cycle distribution at the beginning of each recording, which started 2 hours after drug treatment began, and found a similar cell cycle distribution in vinorelbine and nocodazole-treated cells (15–27% of cells in mitosis for vinorelbine, and 25–37% for nocodazole) (Fig. 2A). The proportion of mitotic cells was not significantly different between these populations ($P=0.09$) (Fig. 2A).

After treatment with vinorelbine, the cell cycle distribution of cells when they entered apoptosis did not differ from the cell cycle distribution of cells at the beginning of the movies, indicating that vinorelbine-induced apoptosis was independent of the cell cycle (Fig. 2A,B; supplementary material Movies 1–6). Nocodazole, like vinorelbine, depolymerizes microtubules but induces cell death primarily during mitosis (Beswick et al., 2006; Brito and Rieder, 2009) and not in interphase (Fig. 1C). Therefore, nocodazole acted as a control for apoptosis induced by prolonged SAC activation (Fig. 2B). Indeed, in our assay we confirmed that cells predominantly died during mitosis, and not in interphase, when treated with nocodazole. This was in stark contrast to results with vinorelbine treatment: when treated with nocodazole only 13–26% of cells entered apoptosis during

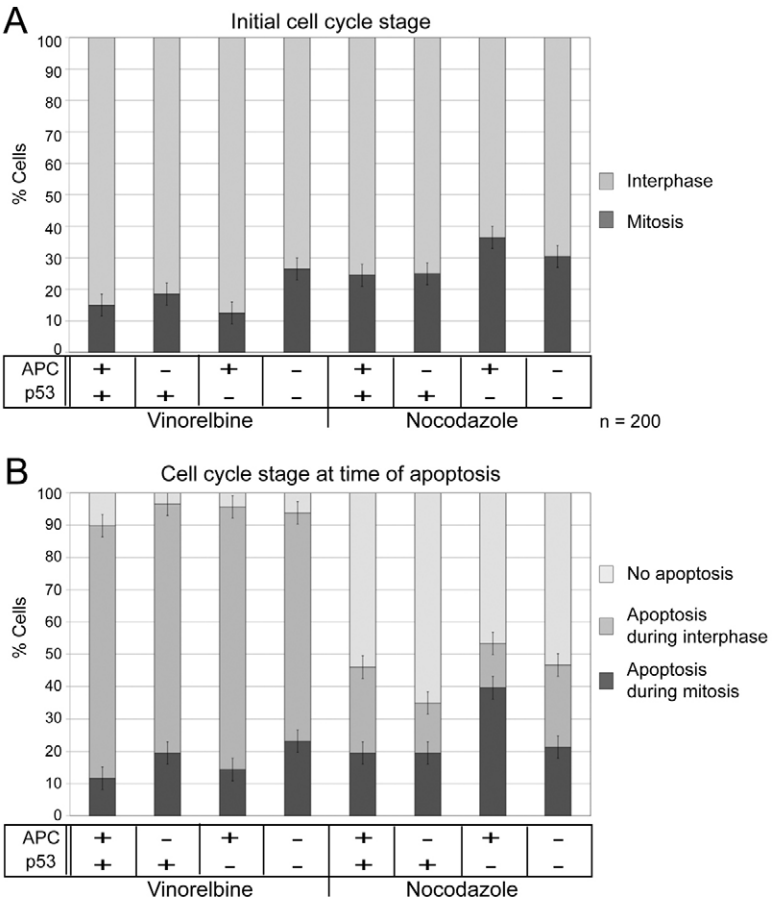

Fig. 2. Cells enter apoptosis directly during interphase when treated with vinorelbine. U2OS cells lacking APC and/or p53, as indicated, and expressing fluorescent lamin B1 to mark the nuclear envelope, were treated with either 50 μg/ml vinorelbine or 1.25 μg/ml nocodazole and followed for 24 hours by fluorescence microscopy in the presence of Nucview. Time-lapse movies were recorded starting 2 hours after vinorelbine or nocodazole treatment. (**A**) Cell cycle distribution after 2 hours of drug treatment. The cell cycle stage of 200 randomly selected cells was scored 2 hours after adding vinorelbine or nocodazole. Mitotic cells were identified by visualiwing vesiculariwation of fluorescent lamin B1 as a marker for nuclear envelope breakdown. The highest standard error is shown as error bars. (**B**) The cell cycle stage immediately before cells entered apoptosis was recorded in the same cells as in A. Cell death was detected using NucView and mitotic cells were scored by visualiwing vesiculariwation of fluorescent lamin B1 (nuclear envelope breakdown) as a marker. Vinorelbine treatment induced cell death significantly more frequently during interphase than nocodazole treatment. ($P=0.0001$). Nocodazole preferentially induced cell death in mitotic cells ($P=0.002$). The probability of entering cell death was not influenced by the initial cell cycle stage in vinorelbine-treated cells ($P=0.26$).

interphase versus 70–82% for vinorelbine ($P<0.0001$) (Fig. 2B). Importantly, our recordings showed that, in nearly all cases, apoptosis that occurred during interphase did not follow mitosis. Thus, vinorelbine appeared to kill cells independently of the cell cycle because the likelihood of a cell entering apoptosis was independent of its cell cycle stage at the beginning of the recording ($P=0.26$) (Fig. 2A,B) and this was independent of APC or p53 status.

Because vinorelbine induced cell death during interphase, we predicted that this drug would kill more cells than nocodazole. This was indeed the case, as shown by the higher overall incidence of cell death after vinorelbine treatment (Fig. 2B). Over the same time period, vinorelbine induced cell death in at least 90% of all cells, whereas nocodazole induced cell death in only 54% of cells, at most, during the 24-hour time-lapse movies (Fig. 2B). Under the same conditions, there was little cell death in cells not exposed to microtubule poisons, regardless of APC or p53 status (data not shown).

APC loss enhances recruitment of the pro-apoptotic protein BIM to mitochondria and this is more pronounced after vinorelbine treatment

Nocodazole and vinorelbine depolymerize microtubules, but only vinorelbine causes the formation of tubulin paracrystals (supplementary material Fig. S2), which have been well characterized (Gigant et al., 2005). This prompted us to test whether differences in responses by microtubule-associated proteins could explain vinorelbine-induced cell death. Specifically, we examined the previously reported microtubule-associated pro-apoptotic protein BIM. BIM inhibits the anti-apoptotic protein BCL2 and also has been reported to be associated with microtubules in a manner dependent on dynein light chain 8 (Puthalakath et al., 1999). Importantly, in response to apoptotic stimuli, BIM translocates to mitochondria, where it can locally inhibit BCL2 (Puthalakath et al., 1999).

The role of BIM as a mediator of apoptosis and its association with microtubules prompted us to investigate whether recruitment of BIM to mitochondria was an early event in vinorelbine-induced apoptosis, and whether APC or p53 status affected such response (Fig. 3). We were unable to detect BIM at microtubules by using immunofluorescence and BIM was not recruited to vinorelbine-induced tubulin paracrystals (supplementary material Fig. S3A). However, BIM protein was slightly more abundant at mitochondria after treatment with vinorelbine but not nocodazole (Fig. 3). Importantly, in each case, the accumulation of BIM at mitochondria was significantly greater in cells lacking APC regardless of p53 status (Fig. 3). Depleting p53 on its own did not have a measurable effect on the localization of BIM to mitochondria (Fig. 3). The increase in mitochondria-associated BIM protein in APC-deficient cells is consistent with the idea that the altered microtubule dynamics in APC-deficient cells changes the ability of BIM to be recruited to mitochondria (Kroboth et al., 2007) (Fig. 3A,B). An increase in total BIM protein could not explain these observations because total BIM protein was reduced in APC deficient cells (Fig. 4A). Our data suggest that the recruitment of BIM to mitochondria contributes to vinorelbine-induced cell death particularly in APC-deficient cells.

The overall ability of vinorelbine to induce cell death during interphase correlated well with the recruitment of BIM to mitochondria: cells lacking APC were killed more readily and

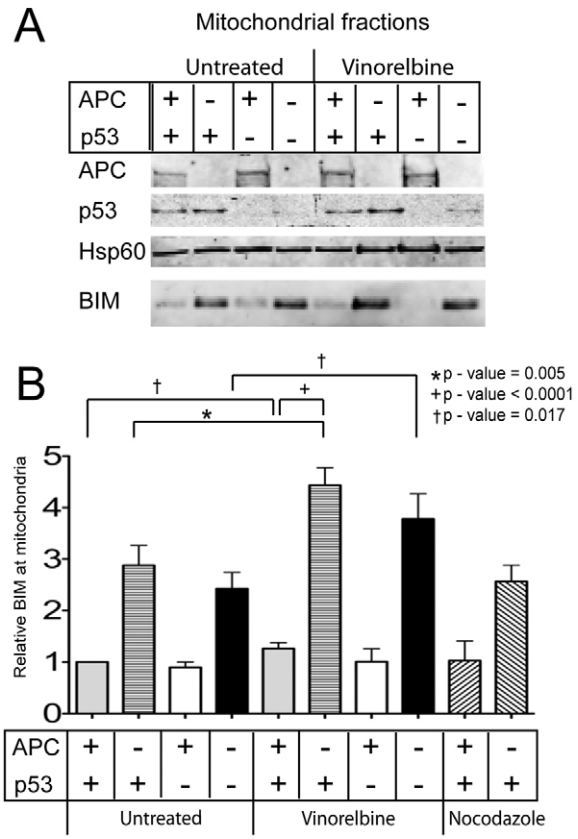

Fig. 3. APC depletion induces the accumulation of BIM in mitochondria, which is enhanced by vinorelbine. (**A**) APC and p53 were depleted by using RNAi. Cells were treated with 10 μg/ml vinorelbine for 30 minutes, harvested and mitochondria extracted. Equal amounts of protein were loaded and mitochondrial enrichment was confirmed using HSP60 as a mitochondrial marker. APC and p53 protein was measured in the same samples. (**B**) Mitochondrial fractions were collected and immunoblotted with the antibodies indicated in A. The relative intensity of bands was measured using an Odyssey LiCor imaging system. HSP60 acted as a mitochondrial marker. BIM levels are shown relative to those in asynchronous, control cells (APC- and p53-positive). At least four independent experiments were performed and the mean of the relative amount of BIM (±s.e.m.).

recruited more BIM to mitochondria (Figs 1, 3). p53 did not affect this recruitment and protected cells instead, suggesting that p53 acts independently of BIM (Figs 3, 4). When treated with 100 μg/ml vinorelbine, more than 37.3% of APC-depleted cells were positive for aCasp3 after 4 hours, compared with 23.3% in control cells. This was slightly enhanced, although not significantly different ($P=0.42$), in cells depleted of both APC and p53 (39.0%) (Fig. 4C). Depleting p53 alone reduced the number of aCasp3-positive cells to 18.8% (Fig. 4C). Together, these results suggest that APC depletion has a dominant effect over p53 depletion in enhancing vinorelbine-induced cell death. Interestingly, compared with control cells, p53-negative cells showed a lower basal level of apoptosis in the absence of vinorelbine ($P<0.03$), whereas APC-, and p53 and APC double-negative cells did not (Fig. 1A,B).

Furthermore, BIM depletion dampened vinorelbine-induced apoptosis in APC-deficient cells, confirming that it contributes to apoptosis induced by vinorelbine (Fig. 4C). When BIM was

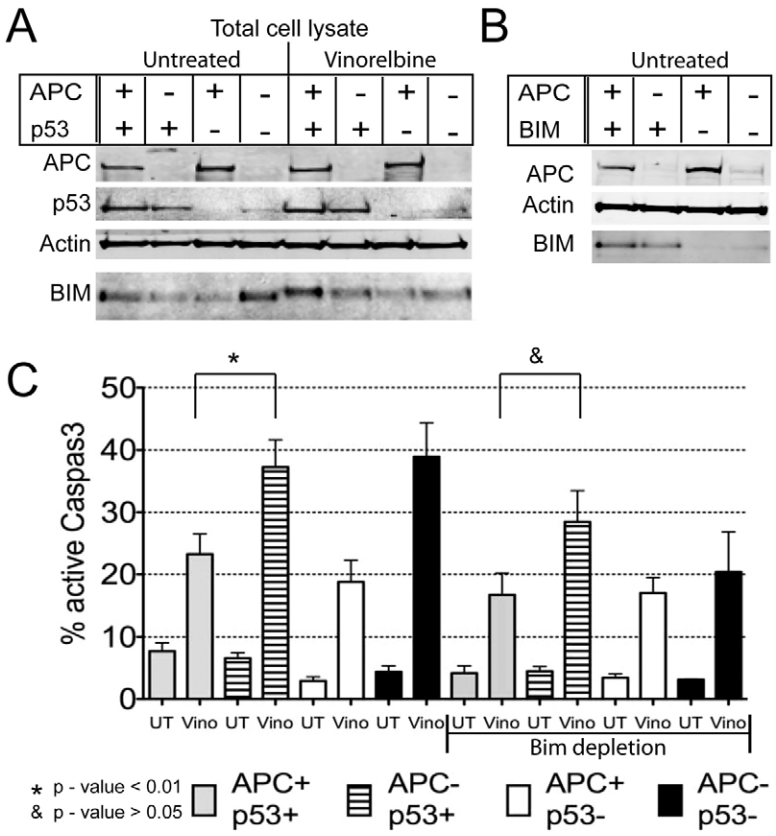

Fig. 4. Increased sensitivity to vinorelbine in APC-deficient cells is not compromised by loss of p53 but is diminished in the absence of BIM. (**A**,**B**) Total cell lysates were immunoblotted to confirm RNAi-mediated depletion of APC, p53 and BIM in control or vinorelbine-treated cells (100 μg/ml, 4 hours) as indicated. Loading of equal amounts of protein was confirmed by measuring the amount of actin. (**C**) BIM-, APC- and/or p53-deficient U2OS cells, as indicated, were treated for 4 hours with 100 μg/ml vinorelbine, fixed with PFA, stained for aCasp3 and analyzed by using flow cytometry. Vinorelbine treatment was performed in three independent experiments in duplicates and for each sample 10,000 cells were analyzed. Results are means±s.e.m. Depleting APC increased the sensitivity to vinorelbine significantly and BIM depletion reduced this effect.

depleted, there was no significant difference in the number of aCasp3-positive cells between either control or p53 deficient cells (17.0%) and cells deficient in both APC and p53 (20.4%) ($P>0.05$, Fig. 4C).

Together these data suggest that the amount of BIM at mitochondria in response to the combined effect of vinorelbine and APC depletion exceeds the threshold that causes sufficient BCL2 inhibition to induce death. In this context, it is important to note that the increased recruitment of BIM to mitochondria does not depend on changes in β-catenin, given that HCT116 colorectal tumour cells, which express mutant β-catenin that is not degraded in response to APC depletion, also exhibit increased sensitivity to vinorelbine and have more BIM at mitochondria when APC is depleted (supplementary material Fig. S4; data not shown).

A correlation between BIM recruitment to mitochondria and interphase cell death is supported by our finding that nocodazole, which kills cells consequent to failed mitosis (Fig. 2B), did not induce BIM recruitment to mitochondria in control and APC-deficient cells (Fig. 3B). This observation also showed that recruitment of BIM to mitochondria is not merely a consequence of microtubule depolymerization (Fig. 3B). Whether the tubulin paracrystals induced by vinorelbine or other changes in free tubulin heterodimers contribute to the recruitment of BIM to mitochondria will require future investigation.

Vinorelbine induces cell death in adenoma in vivo

To determine whether the enhanced sensitivity to vinorelbine in cultured cells lacking APC was also true for cells in tissue, we administered vinorelbine to $APC^{Min/+}$ mutant mice with adenoma (which lack full-length APC) and compared the response of the adenoma tissue with that of physiologically normal tissue (which retains the wild-type APC allele) (Fig. 5). To determine the relationship between mitotic arrest and vinorelbine-induced death in cells in situ, we counted the number of apoptotic cells in the intestine of mice at various times after they were injected with vinorelbine or taxol (Fig. 5A,B). Just as in cultured cells, vinorelbine induced cell death in intestinal epithelial cells within 30 minutes after treatment, whereas tissue from taxol-treated animals only contained increased numbers of apoptotic cells 6 hours after treatment (Fig. 5A,B). Furthermore, in taxol-treated tissue, the appearance of apoptotic cells only occurred after mitotically arrested cells had accumulated, confirming that killing by taxol, but not vinorelbine, follows mitotic arrest (Fig. 5A,B). Consistent with the increased response in APC-deficient cells, vinorelbine induced apoptosis over threefold more efficiently in adenoma than in normal tissue when corresponding regions in the same animal were compared (Fig. 5C,D). Consistent with a defect in mitotic arrest in APC-deficient cells, cells in normal tissue arrested more efficiently in mitosis than cells in adenoma (Fig. 5E). Importantly, the increased sensitivity of APC-deficient cells to vinorelbine translated into a significantly reduced adenoma size in $APC^{Min/+}$ mice ($P=0.0001$) (Fig. 5F).

These results strongly suggest that vinorelbine could be a useful treatment for colorectal cancers with APC mutations.

Discussion

The effectiveness of currently available chemotherapy for advanced colorectal cancer is limited, making the identification

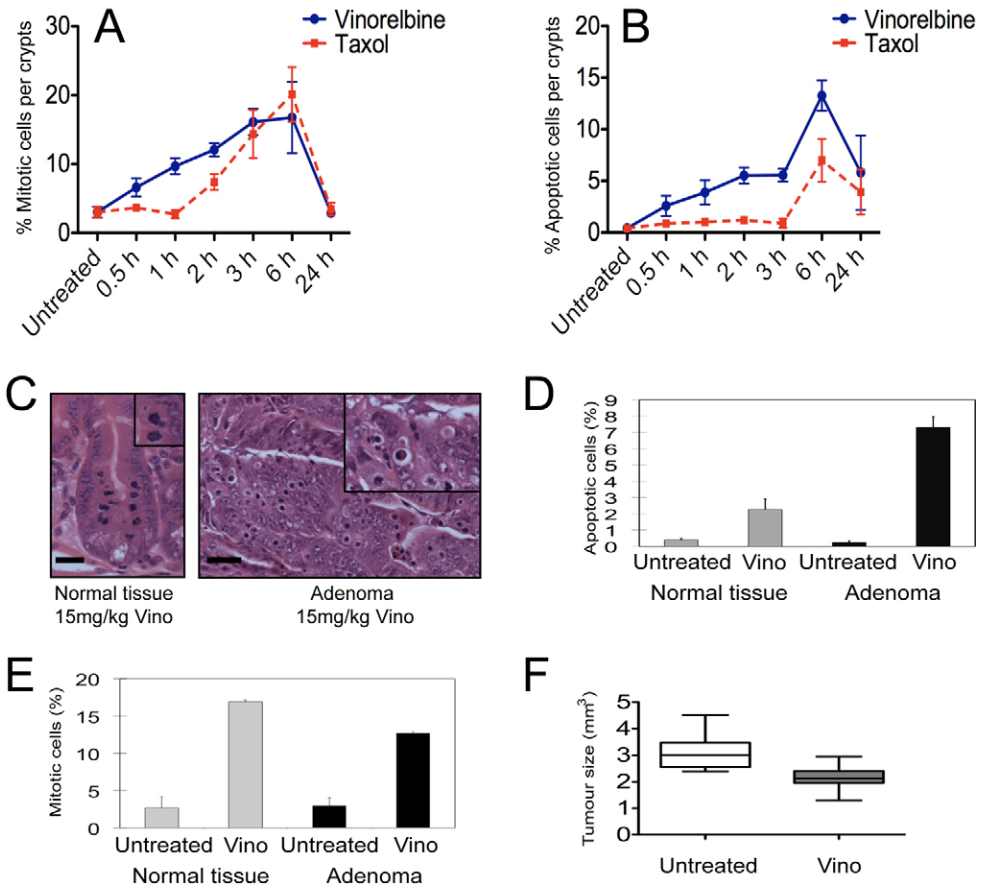

Fig. 5. Vinorelbine kills cells during interphase in situ. Wild-type mice were injected with 10 mg per kg of body weight vinorelbine or taxol and tissue was harvested at the indicated times and processed for H&E staining (Radulescu et al., 2010). Mitotic (**A**) and apoptotic figures (**B**) were counted in 25 crypts in at least three mice. Their number per crypt is plotted for each time point. Vinorelbine treatment resulted in the appearance of apoptotic cells within 30 minutes, whereas taxol-treated tissue had an accumulation of mitotic cells before the appearance of apoptotic cells. In addition, significantly elevated apoptosis was still detectable in vinorelbine-treated tissue at 24 hours, but this had dropped almost to background in taxol-treated tissue. (**C**–**E**) Vinorelbine induces cell death preferentially in APC-deficient adenoma and mitotic arrest in normal tissue. Wild-type or $APC^{Min/+}$ mice were treated with 15 mg per kg of body weight vinorelbine for 6 hours, and tissue was harvested and processed for H&E staining. (C) Example images of a wild-type crypt on the left and an adenoma on the right, with insets showing selected apoptotic cells (enlarged 1.8-fold). Scale bars: 20 µm. Apoptotic (D) and mitotic (E) cells were counted in 5 tumours for each type from three mice ($APC^{Min/+}$) or 25 crypts each in three mice (wild type). (**F**) Vinorelbine reduces adenoma size in APC-deficient adenoma. $APC^{Min/+}$ mice (45–50 days old) were injected once every 2 weeks with 10 mg per kg of body weight vinorelbine or vehicle. Intestines were harvested at a 90-day timepoint and tumour burden was scored on wholemount tissue by measuring tumour number and size.

of suitable targets for this common human cancer an important goal (Segal and Saltz, 2009). Because most colorectal cancer cells carry APC mutations, and in line with the concomitant decrease in microtubule stability, we considered the possibility that treatment of colorectal cancer with microtubule poisons is a potentially useful approach.

However, we had previously found that APC-deficient cells died less readily than cells with normal levels of APC, owing to impaired mitotic arrest, when treated with taxol and nocodazole (Dikovskaya et al., 2007). This encouraged us to investigate further how another microtubule poison vinorelbine, which is currently used as a chemotherapeutic drug, produces cell death. To the best of our knowledge, vinorelbine has not been considered for therapy in colorectal cancer. Here, we report the potential usefulness of vinorelbine as chemotherapeutic for APC-deficient and colorectal cancer cells.

We discovered that vinorelbine kills cells independently of the cell cycle, showing for the first time that vinorelbine-induced cell death is not simply a consequence of prolonged mitotic arrest (Figs 1, 2, 4, 5). This was true in tissue in mice treated with vinorelbine (Fig. 5) and in cells (Figs 1, 2, 4). Time-lapse movies showed that cells enter apoptosis as a result of vinorelbine treatment during the cell cycle stage in which they first encountered the drug (Fig. 2). Our analysis showed that interphase death did not follow mitotic slippage (Fig. 2; supplementary material Fig. S1). These findings demonstrate that vinorelbine can induce cell death during interphase and does not rely on mitotic arrest.

We chose to examine the contributions of two of the most prevalent colorectal cancer mutations, APC and p53, to this process (Figs 2–4). APC mutations are early events in tumorigenesis, whereas mutations in p53 tend to occur later. Both have also been implicated in death following mitotic arrest (Chi et al., 2009; Dikovskaya et al., 2007). Our results showed that loss of APC (depletion or mutation) renders cells more sensitive to vinorelbine-induced apoptosis (Fig. 1A; supplementary material Fig. S4A), whereas loss of p53 was slightly protective, suggesting that APC acts either downstream

or independently of p53, given that p53 loss had no effect on the phenotype resulting from APC loss (Figs 2,4). Our finding that two relatively well-differentiated colorectal tumour cells lines (DLD1 and Caco-2) are killed more effectively by vinorelbine compared with cells expressing wild-type APC further supports our idea that APC mutant cells could be potentially selectively targeted by this agent. By contrast, more heterogeneous, generally less-differentiated SW480 cells responded to vinorelbine in a similar manner to cells expressing wild-type APC (supplementary material Fig. S4A). This suggests that more advanced tumours might not retain sensitivity to vinorelbine. However, a more detailed analysis will be required to identify all the required parameters that govern and predict sensitivity to vinorelbine.

Some p53 and APC protein co-fractionated with mitochondria, suggesting that their anti-apoptotic function might involve mitochondrial processes (Brocardo et al., 2008; Marchenko et al., 2000). To examine the relationship between the changes induced by microtubule poisons and the mitochondrial recruitment of known apoptotic regulators, we chose to investigate BIM in this context (Figs 3, 4). BIM has been described as a microtubule-bound, pro-apoptotic factor that is recruited to mitochondria to induce cell death through the inhibition of the key anti-apoptotic protein BCL2 (Merino et al., 2009; Puthalakath et al., 1999).

Vinorelbine treatment on its own induced some recruitment of BIM to mitochondria in control cells, whereas nocodazole did not (Fig. 3B). Most importantly, this effect of vinorelbine was significantly increased in APC-depleted cells but not in cells lacking p53 (Fig. 3A,B). Overall cellular BIM protein levels were not affected by altered APC expression (Fig. 4A). This suggested that APC-deficiency might prime cells for apoptosis by increasing the amount of BIM at mitochondria as a response to microtubule stress. These and previously published data suggest that the reduced microtubule stability in APC mutant cells enhances recruitment of BIM to mitochondria, possibly because of a reduction in the association of BIM with microtubules. Alternatively, APC could affect the association of BIM with mitochondrial proteins. The idea that other APC interactions contribute to the effects we observe is supported by our finding that cells that express only truncated fragments of APC, which are not thought to contribute to microtubule stability, are also more efficiently killed by vinorelbine when the truncated APC fragment is removed (supplementary material Fig. S4B). For instance, DLD1 and SW480 cells are killed more readily when APC has been depleted (supplementary material Fig. S4B). In HCT116 and SW480 cells, the increased killing is accompanied by increased BIM at mitochondria (data not shown). These data suggest that domains in N-terminal regions of APC directly contribute to events at mitochondria that affect apoptosis, consistent with the previous findings that N-terminal fragments of APC localize to mitochondria in tumour cells (Brocardo et al., 2008). These data, together with the increased sensitivity of colorectal tumour cells to vinorelbine, also suggest that changes in β-catenin or Wnt signalling are not required for the sensitivity to vinorelbine.

Another observation was that vinorelbine induced an increase in the apparent molecular weight of BIM, consistent with its phosphorylation. This was reduced in APC- and/or p53-deficient cells (Fig. 4A), suggesting that this post-translational modification has a protective role. However, in the absence of additional detailed information about the role of post-translational modification for the function of BIM, this is purely speculative.

Our data show that vinorelbine kills cells by different mechanisms than that of other microtubule poisons. Vinorelbine induces tubulin paracrystals and acts on interphase microtubules, which might be linked to this phenomenon (Lobert et al., 1998; Verdier-Pinard et al., 1999; Jean-Decoster et al., 1999) (supplementary material Fig. S2). Therefore we examined the association of microtubule-binding proteins with tubulin paracrystals in vinorelbine-treated cells. The paracrystals colocalized with acetylated tubulin, MAP2, EB1 (also known as MAPRE1), Clip170 (also known as CLIP1) and APC, only a little with CLASP1, and not at all with BCL2 and BIM (supplementary material Figs S2, S3). This raises the possibility that paracrystals sequester a subset of microtubule-binding proteins, competing them away from other locations in the cell, to invoke cellular changes that could promote cell death. Another possibility is that different modifications of tubulin itself contribute to the difference between the actions of vinorelbine and other microtubule poisons (supplementary material Fig. S2). For instance, a cellular sensor for free tubulin might be activated in cells treated with nocodazole, but not vinorelbine, owing to the sequestration of tubulin into paracrystals by the latter but not the former. How cells sense free versus polymerized tubulin remains unclear. Vinca alkaloids induce transcription of β3 tubulin (Bachurski et al., 1994; Saussede-Aim et al., 2009), and the ability of β-tubulin to regulate the stability of its mRNA (Bachurski et al., 1994) might be affected by vinorelbine. This might, in turn, have consequences that contribute to cell death and other cellular responses.

Importantly, the increased sensitivity of APC mutant cells to vinorelbine was measurable in murine adenomas lacking APC and in colorectal tumour cells (Fig. 5; supplementary material Fig. S4B). This observation reveals vinorelbine as a potentially useful chemotherapeutic for colorectal cancer. The details of how changes in APC expression contribute to the sensitivity of cells to vinorelbine, and how loss of p53 attenuates this effect, will require further investigation. Nevertheless, an important conclusion from our data is that the genotype of cells for these two commonly mutated tumour suppressor proteins, APC and p53, could be crucial when deciding how to treat colorectal tumours and has important implications for personalized cancer therapy.

Materials and Methods

Cell culture and drug treatment

Human osteosarcoma (U2OS) cells were obtained from Cancer Research UK, cultured in DMEM supplemented with 10% FBS, 1% penicillin–streptomycin stock solution (Life Technologies) and nonessential amino acids at a dilution of 1:100 (Sigma-Aldrich). For siRNA-mediated protein depletion, U2OS cells were transfected using INTERFERin (Polyplus) according to the manufacturer's instructions with 10 nM siRNAs targeting human APC and/or p53 (Qiagen), or a non-targeted control (Dharmacon) as described previously (Dikovskaya et al., 2007). For live-cell fluorescence markers, U2OS cells were co-transfected with 0.2 μg DNA encoding mCherry-tagged lamin B1 along with 10 nM APC and/or p53 siRNAs (Dharmacon, Qiagen) using Fugene 6 (Roche) according to the manufacturer's instructions. NucView (Biotium) was added to medium to detect caspase-3 activation as described previously (Cen et al., 2008). To induce mitotic arrest and cell death, U2OS cells were treated with 1.5 μg/ml nocodazole or various concentrations of vinorelbine (see figure legends). To determine BCL2 localization upon vinorelbine treatment, U2OS cells were co-transfected with 0.2 μg DNA encoding mCherry–tubulin (a kind gift from Markus Posch, University of Dundee, Dundee, UK) and 0.4 μg DNA encoding GFP–BCL2 (Wang et al., 2001).

Microscopy and immunofluorescence

Cells were fixed in a warm solution of 1.8% PFA in PHEM buffer (60 mM Pipes pH 6.9, 4 mM $MgSO_4$, 25 mM Hepes and 10 mM K-EGTA) for 15 minutes at 37℃, washed in PBS, and blocked in blocking buffer (0.1% Triton X-100, 2% BSA, 5% donkey serum, 0.02% NaN_3 in PBS supplemented with 50 mM NH_4Cl, for fixation only) for 1 hour. Primary antibodies against the following proteins were diluted in blocking buffer as follows: supernatant from hybridoma cells producing anti-tubulin antibody (YL1/2) at 1:25; BIM (AbCam) at 1:100; Clip170 at 1:300 [kindly provided by Niels Galjart (Tanenbaum et al., 2008), pericentrin (AbCam) at 1:2500, INCENP and KAP3 (BD Transduction Laboratories) at 1:200, EB1 (Transduction Laboratories) at 1:50, MAP2 (Sigma-Aldrich) was at 1:300; and anti-M-APC polyclonal (Näthke et al., 1996) at 1:500. For CLASP1 staining, cells were fixed in −20℃ methanol for 10 minutes and then processed as described above for PFA fixation with no NH_4Cl in the blocking buffer. The antibody against CLASP1 (kind gift from Fedor Severin) was diluted 1:300 in blocking buffer. Secondary antibodies raised in donkey were conjugated to Alexa Fluor 488, Alexa Fluor 568 or Alexa Fluor 647 (Invitrogen), and were diluted 1:1000 in blocking buffer. Cells were counterstained with DAPI at 1 µg/ml for 20 minutes. High-resolution images were collected with a Delta-Vision Restoration imaging system (Applied Precision, Issaquah, WA) based on an Olympus IX70 inverted microscope stand, using a 100× 1.4NA objective lens. Images were acquired at 0.25 µm *Z*-intervals and recorded with CoolSnap CCD camera (Roper Scientific). Images were deconvolved and three-dimensionally rendered using SoftWoRx software (Applied Precision).

Lamin B1 and Nucview time-lapse movies were collected using a Nikon Eclipse Ti-E inverted microscope, a 40× 1.4 NA objective lens and a Photometrics Cascade EM-CCD camera. To acquire a time-lapse movie, an image was collected every 15 minutes for 24 hours, with the first time-point occurring 2 hours after 50 µg/ml vinorelbine treatment. Cells were kept at 37℃ and under 5% CO_2 throughout the recording. Movies and images were analysed using ImageJ (http://rsb.info.nih.gov/ij/).

Immunoblotting

Mitochondrial isolation was performed using the AbCam Cytochrome C Releasing Apoptosis Assay Kit according to the manufacturer's instructions. Total protein concentration was measured using the Bradford Assay (BioRad) according to the manufacturer's instructions, to ensure equal protein loading on SDS-PAGE gels. We used the following proteins (the antibody is given in brackets) as loading controls: HSP60 (CST) for mitochondrial fractions, and tubulin (YL1/2), actin (C4 clone; MP Biomedicals) and glyceraldehyde 3-phosphate dehydrogenase (GAPDH; AbCam) for cytoplasmic proteins. Immunoblots were imaged and quantified with the LICOR Odyssey imaging system. To quantify protein amounts, the signal intensity for a protein was normalized to the signal intensity of an appropriate loading control in the same sample. Reported protein levels are relative to the control treatment, which was used as a reference in each individual experiment.

For total protein lysis, cells were lysed in MEBC buffer (50 mM Tris-HCl pH 7.5, 100 mM NaCl, 5 mM EGTA, 5 mM EDTA, 0.5% NP-40, and 40 mM 2-glycerophosphate) supplemented with 10 µg/ml each of leuptin, pepstatin A and chymotrypsin (Peptide Institute, Inc.). Lysate was collected using cell scrapers and was then centrifuged (20 minutes, 20,000 ***g***, 4℃). Supernatant was run on NuPage 4–12% gradient SDS-PAGE gels (Invitrogen) using MOPS running buffer (Invitrogen). The separated proteins were transferred onto a nitrocellulose membrane (Protran BA 79) with a 0.1 µm pore size (Whatman). Antibodies were diluted in blocking buffer (TBS containing 5% nonfat milk powder, 1% donkey serum and 0.02% Triton X-100) as follows: anti-APC and ALI mouse monoclonal antibody [against the N terminus; Cancer Research UK (Efstathiou et al., 1998) or crude serum of rabbit polyclonal antibody raised against the N-terminus of APC (anti-N-APC antibody) (Midgley et al., 1997), 1:1000; anti-α-tubulin rat monoclonal antibody (YL1/2), 1:100; anti-actin antibody, 1:500; anti-GAPDH antibody (AbCam), 1:2000; anti-BIM (AbCam) mouse monoclonal antibody, 1:1000; anti-p53 DO-1 mouse monoclonal antibody, 1:1000; and anti-HSP60 (CST) antibody, 1:1000. Secondary anti-rabbit, -mouse or -rat IRDye-800/680-conjugated antibodies (Rockland and Invitrogen) were diluted 1:5000 in blocking buffer.

Flow cytometry

To detect aCasp3, cells were fixed and stained using the aCasp3 phycoerythrin (PE) monoclonal antibody apoptosis kit (BD Biosciences) according to the manufacturer's instructions. In brief, cells were collected and fixed in 1% PFA on ice for 20 minutes and then washed in Saponin solution. The cell profile was analyzed on a flow cytometer (FACSCalibur; Becton Dickinson) using CellQuest Pro software (BD Biosciences). Data analysis was performed using Flowjo software (Tree Star).

Statistical analysis

Statistical significance between sample means was calculated using the Student's *t* test (using Graphpad Prism V5.0b).

Animal tissue

Wild type or $APC^{Min/+}$ mice were injected intravenously with 10 mg per kg of body weight vinorelbine or 10 mg per kg of body weight taxol intraperitoneally (Radulescu et al., 2010). Tissue was harvested at the indicated times for the timecourse comparison (Fig. 3). Tissue was prepared and apoptosis and mitotic figures scored as previously described (Sansom et al., 2004; Cole et al., 2010) for five tumours each in $APC^{Min/+}$ mouse or for 25 crypts in three wild-type controls. To measure tumour size in $APC^{Min/+}$ mice, animals (45–50 days old) were injected once every 2 weeks with 10 mg per kg of body weight vinorelbine or vehicle. Tissue was harvested at 90 days and prepared for H&E staining, and the size of the indicated number of tumours was measured as described previously (Radulescu et al., 2010). All animal experiments were performed under the UK Home Office Guidelines.

Acknowledgements

We are grateful to all those who supplied reagents and have indicated this in the text. We thank R. J. S. Steele (Molecular Surgery, University of Dundee) for critical reading of the manuscript and members of the Näthke lab for helpful discussions.

Funding

This work was supported by funding from Cancer Research UK to I.S.N. and O.J.S. [grant numbers C430/A11243, A430/A6811, C696/A10419]; Association for International Cancer Research (AICR) to O.J.S. [grant number 06-0614]; and the Wellcome Trust to D.M.K. [grant number 083923/Z/07/Z]. The authors do not have any conflict of interest to report for this study. Deposited in PMC for release after 6 months.

Supplementary material available online at
http://jcs.biologists.org/lookup/suppl/doi:10.1242/jcs.091843/-/DC1

References

Bachurski, C. J., Theodorakis, N. G., Coulson, R. M. and Cleveland, D. W. (1994). An amino-terminal tetrapeptide specifies cotranslational degradation of beta-tubulin but not alpha-tubulin mRNAs. *Mol. Cell. Biol.* **14**, 4076-4086.

Beswick, R. W., Ambrose, H. E. and Wagner, S. D. (2006). Nocodazole, a microtubule depolymerising agent, induces apoptosis of chronic lymphocytic leukaemia cells associated with changes in Bcl-2 phosphorylation and expression. *Leuk. Res.* **30**, 427-436.

Bourgarel-Rey, V., Savry, A., Hua, G., Carré, M., Bressin, C., Chacon, C., Imbert, J., Braguer, D. and Barra, Y. (2009). Transcriptional down-regulation of Bcl-2 by vinorelbine: identification of a novel binding site of p53 on Bcl-2 promoter. *Biochem. Pharmacol.* **78**, 1148-1156.

Brito, D. A. and Rieder, C. L. (2009). The ability to survive mitosis in the presence of microtubule poisons differs significantly between human nontransformed (RPE-1) and cancer (U2OS, HeLa) cells. *Cell Motil. Cytoskeleton* **66**, 437-447.

Brocardo, M., Lei, Y., Tighe, A., Taylor, S. S., Mok, M. T. S. and Henderson, B. R. (2008). Mitochondrial targeting of adenomatous polyposis coli protein is stimulated by truncating cancer mutations: regulation of Bcl-2 and implications for cell survival. *J. Biol. Chem.* **283**, 5950-5959.

Castedo, M., Perfettini, J.-L., Roumier, T., Andreau, K., Medema, R. and Kroemer, G. (2004). Cell death by mitotic catastrophe: a molecular definition. *Oncogene* **23**, 2825-2837.

Cen, H., Mao, F., Aronchik, I., Fuentes, R. J. and Firestone, G. L. (2008). DEVD-NucView488: a novel class of enzyme substrates for real-time detection of caspase-3 activity in live cells. *FASEB J.* **22**, 2243-2252.

Chen, T., Yang, I., Irby, R., Shain, K. H., Wang, H. G., Quackenbush, J., Coppola, D., Cheng, J. Q. and Yeatman, T. J. (2003). Regulation of caspase expression and apoptosis by adenomatous polyposis coli. *Cancer Res.* **63**, 4368-4374.

Chi, Y.-H., Ward, J. M., Cheng, L. I., Yasunaga, J. and Jeang, K.-T. (2009). Spindle assembly checkpoint and p53 deficiencies cooperate for tumorigenesis in mice. *Int. J. Cancer* **124**, 1483-1489.

Cole, A. M., Ridgway, R. A., Derkits, S. E., Parry, L., Barker, N., Clevers, H., Clarke, A. R. and Sansom, O. J. (2010). p21 loss blocks senescence following Apc loss and provokes tumourigenesis in the renal but not the intestinal epithelium. *EMBO Mol. Med.* **2**, 472-486.

Conroy, T. (2002). Activity of vinorelbine in gastrointestinal cancers. *Crit. Rev. Oncol. Hematol.* **42**, 173-178.

Degardin, M., Bonneterre, J., Hecquet, B., Pion, J M., Adenis, A., Horner, D. and Demaille A. (1994). Vinorelbine (navelbine) as a salvage treatment for advanced breast cancer. *Ann. Oncol.* **5**, 423-426.

Dikovskaya, D., Schiffmann, D., Newton, I. P., Oakley, A., Kroboth, K., Sansom, O., Jamieson, T. J., Meniel, V., Clarke, A. and Näthke, I. S. (2007). Loss of APC induces polyploidy as a result of a combination of defects in mitosis and apoptosis. *J. Cell Biol.* **176**, 183-195.

Efstathiou, J. A., Noda, M., Rowan, A., Dixon, C., Chinery, R., Jawhari, A., Hattori, T., Wright, N. A., Bodmer, W. F. and Pignatelli, M. (1998). Intestinal trefoil factor controls the expression of the adenomatous polyposis coli-catenin and the E-cadherin-catenin complexes in human colon carcinoma cells. *Proc. Natl. Acad. Sci. USA* **95**, 3122-3127.

Ellis, G. K., Gralow, J. R., Pierce, H. I., Williams, M. A. and Livingston, R. B. (1999). Infusional paclitaxel and weekly vinorelbine chemotherapy with concurrent filgrastim for metastatic breast cancer: high complete response rate in a phase I-II study of doxorubicin-treated patients. *J. Clin. Oncol.* **17**, 1407-1412.

Fodde, R., Kuipers, J., Rosenberg, C., Smits, R., Kielman, M., Gaspar, C., van Es, J. H., Breukel, C., Wiegant, J., Giles, R. H. et al. (2001). Mutations in the APC tumour suppressor gene cause chromosomal instability. *Nat. Cell Biol.* **3**, 433-438.

Gascoigne, K. E. and Taylor, S. S. (2008). Cancer cells display profound intra- and interline variation following prolonged exposure to antimitotic drugs. *Cancer Cell* **14**, 111-122.

Gigant, B., Wang, C., Ravelli, R. B., Roussi, F., Steinmetz, M. O., Curmi, P. A., Sobel, A. and Knossow M. (2005). Structural basis for the regulation of tubulin by vinblastine. *Nature* **435**, 519-522.

Gonzalez-Cid, M., Larripa, I. and Slavutsky, I. (1997). Vinorelbine: cell cycle kinetics and differential sensitivity of human lymphocyte subpopulations. *Toxicol. Lett.* **93**, 171-176.

Huang, H.-C., Shi, J., Orth, J. D. and Mitchison, T. J. (2009). Evidence that mitotic exit is a better cancer therapeutic target than spindle assembly. *Cancer Cell* **16**, 347-358.

Jean-Decoster, C., Brichese, L., Barret, J. M., Tollon, Y., Kruczynski, A., Hill, B. T. and Wright, M. (1999). Vinflunine, a new vinca alkaloid: cytotoxicity, cellular accumulation and action on the interphasic and mitotic microtubule cytoskeleton of PtK2 cells. *Anticancer Drugs* **10**, 537-543.

Jordan, M. A. and Wilson, L. (2004). Microtubules as a target for anticancer drugs. *Nat. Rev. Cancer* **4**, 253-265.

Jordan, M. A. and Kamath, K. (2007). How do microtubule-targeted drugs work? An overview. *Curr. Cancer Drug Targets* **7**, 730-742.

Kinzler, K. W., Nilbert, M. C., Su, L. K., Vogelstein, B., Bryan, T. M., Levy, D. B., Smith, K. J., Preisinger, A. C., Hedge, P. and McKechnie, D. (1991). Identification of FAP locus genes from chromosome 5q21. *Science* **253**, 661-665.

Kita, K., Wittmann, T., Nathke, I. S. and Waterman-Storer, C. M. (2006). Adenomatous polyposis coli on microtubule plus ends in cell extensions can promote microtubule net growth with or without EB1. *Mol. Biol. Cell* **17**, 2331-2345.

Kroboth, K., Newton, I. P., Kita, K., Dikovskaya, D., Zumbrunn, J., Waterman-Storer, C. M. and Näthke, I. S. (2007). Lack of adenomatous polyposis coli protein correlates with a decrease in cell migration and overall changes in microtubule stability. *Mol. Biol. Cell* **18**, 910-918.

Letai, A. G. (2008). Diagnosing and exploiting cancer's addiction to blocks in apoptosis. *Nat. Rev. Cancer* **8**, 121-132.

Liu, J., Prunuske, A. J., Fager, A. M. and Ullman, K. S. (2003). The COPI complex functions in nuclear envelope breakdown and is recruited by the nucleoporin Nup153. *Dev. Cell* **5**, 487-498.

Lobert, S., Ingram, J. W., Hill, B. T. and Correia, J. J. (1998). A comparison of thermodynamic parameters for vinorelbine- and vinflunine-induced tubulin self-association by sedimentation velocity. *Mol. Pharmacol.* **53**, 908-915.

Marchenko, N. D., Zaika, A. and Moll, U. M. (2000). Death signal-induced localization of p53 protein to mitochondria. A potential role in apoptotic signaling. *J. Biol. Chem.* **275**, 16202-16212.

Merino, D., Giam, M., Hughes, P. D., Siggs, O. M., Heger, K., O'Reilly, L. A., Adams, J. M., Strasser, A., Lee, E. F., Fairlie, W. D. et al. (2009). The role of BH3-only protein Bim extends beyond inhibiting Bcl-2-like prosurvival proteins. *J. Cell Biol.* **186**, 355-362.

Midgley, C. A., White, S., Howitt, R., Save, V., Dunlop, M. G., Hall, P. A., Lane, D. P., Wyllie, A. H. and Bubb, V. J. (1997). APC expression in normal human tissues. *J. Pathol.* **181**, 426-433.

Näthke, I. S., Adams, C. L., Polakis, P., Sellin, J. H. and Nelson, W. J. (1996). The adenomatous polyposis coli tumor suppressor protein localizes to plasma membrane sites involved in active cell migration. *J. Cell Biol.* **134**, 165-179.

Perez, E. A. (2009). Microtubule inhibitors: Differentiating tubulin-inhibiting agents based on mechanisms of action, clinical activity, and resistance. *Mol. Cancer Ther.* **8**, 2086-2095.

Puthalakath, H., Huang, D. C., O'Reilly, L. A., King, S. M. and Strasser, A. (1999). The proapoptotic activity of the Bcl-2 family member Bim is regulated by interaction with the dynein motor complex. *Mol. Cell* **3**, 287-296.

Radulescu, S., Ridgway, R. A., Appleton, P., Kroboth, K., Patel, S., Woodgett, J., Taylor, S., Nathke, I. S. and Sansom, O. J. (2010). Defining the role of APC in the mitotic spindle checkpoint in vivo: APC-deficient cells are resistant to Taxol. *Oncogene* **29**, 6418-6427.

Sansom, O. J., Reed, K. R., Hayes, A. J., Ireland, H., Brinkmann, H., Newton, I. P., Batlle, E., Simon-Assmann, P., Clevers, H., Nathke, I. S. et al. (2004). Loss of Apc in vivo immediately perturbs Wnt signaling, differentiation, and migration. *Genes Dev.* **18**, 1385-1390.

Saussede-Aim, J., Matera, E. L., Herveau, S., Rouault, J. P., Ferlini, C. and Dumontet, C. (2009). Vinorelbine induces beta3-tubulin gene expression through an AP-1 Site. *Anticancer Res.* **29**, 3003-3009.

Segal, N. H. and Saltz, L. B. (2009). Evolving treatment of advanced colon cancer. *Annu. Rev. Med.* **60**, 207-219.

Tanenbaum, M. E., Macurek, L., Galjart, N. and Medema, R. H. (2008). Dynein, Lis1 and CLIP-170 counteract Eg5-dependent centrosome separation during bipolar spindle assembly. *EMBO J.* **27**, 3235-3245.

Uppal, S. O., Li, Y., Wendt, E., Cayer, M. L., Barnes, J., Conway, D., Boudreau, N. and Heckman, C. A. (2007). Pattern analysis of microtubule-polymerizing and -depolymerizing agent combinations as cancer chemotherapies. *Int. J. Oncol.* **31**, 1281-1291.

Varetti, G. and Musacchio, A. (2008). The spindle assembly checkpoint. *Curr. Biol.* **18**, 591-595.

Verdier-Pinard, P., Garès, M. and Wright, M. (1999). Differential in vitro association of vinca alkaloid-induced tubulin spiral filaments into aggregated spirals. *Biochem. Pharmacol.* **58**, 959-971.

Wang, N. S., Unkila, M. T., Reineks, E. Z. and Distelhorst, C. W. (2001). Transient expression of wild-type or mitochondrially targeted Bcl-2 induces apoptosis, whereas transient expression of endoplasmic reticulum-targeted Bcl-2 is protective against Bax-induced cell death. *J. Biol. Chem.* **276**, 44117-44128.

Zumbrunn, J., Kinoshita, K., Hyman, A. A. and Näthke, I. S. (2001). Binding of the adenomatous polyposis coli protein to microtubules increases microtubule stability and is regulated by GSK3 beta phosphorylation. *Curr. Biol.* **11**, 44-49.

Journal of Cell Science

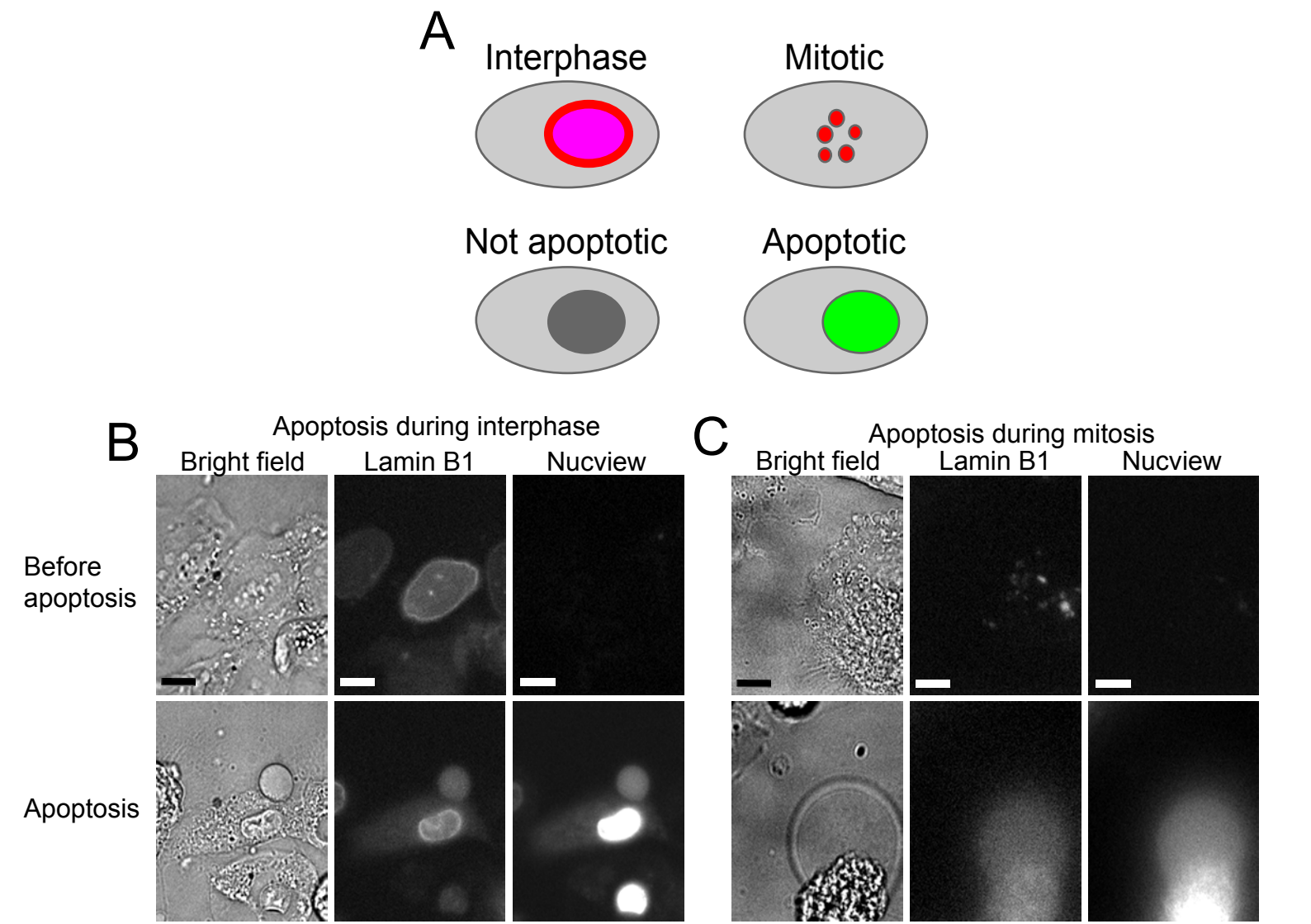
A
Interphase
Mitotic
Not apoptotic
Apoptotic
B
Apoptosis during interphase
Bright field
Lamin B1
Nucview
Before apoptosis
Apoptosis
C
Apoptosis during mitosis
Bright field
Lamin B1
Nucview

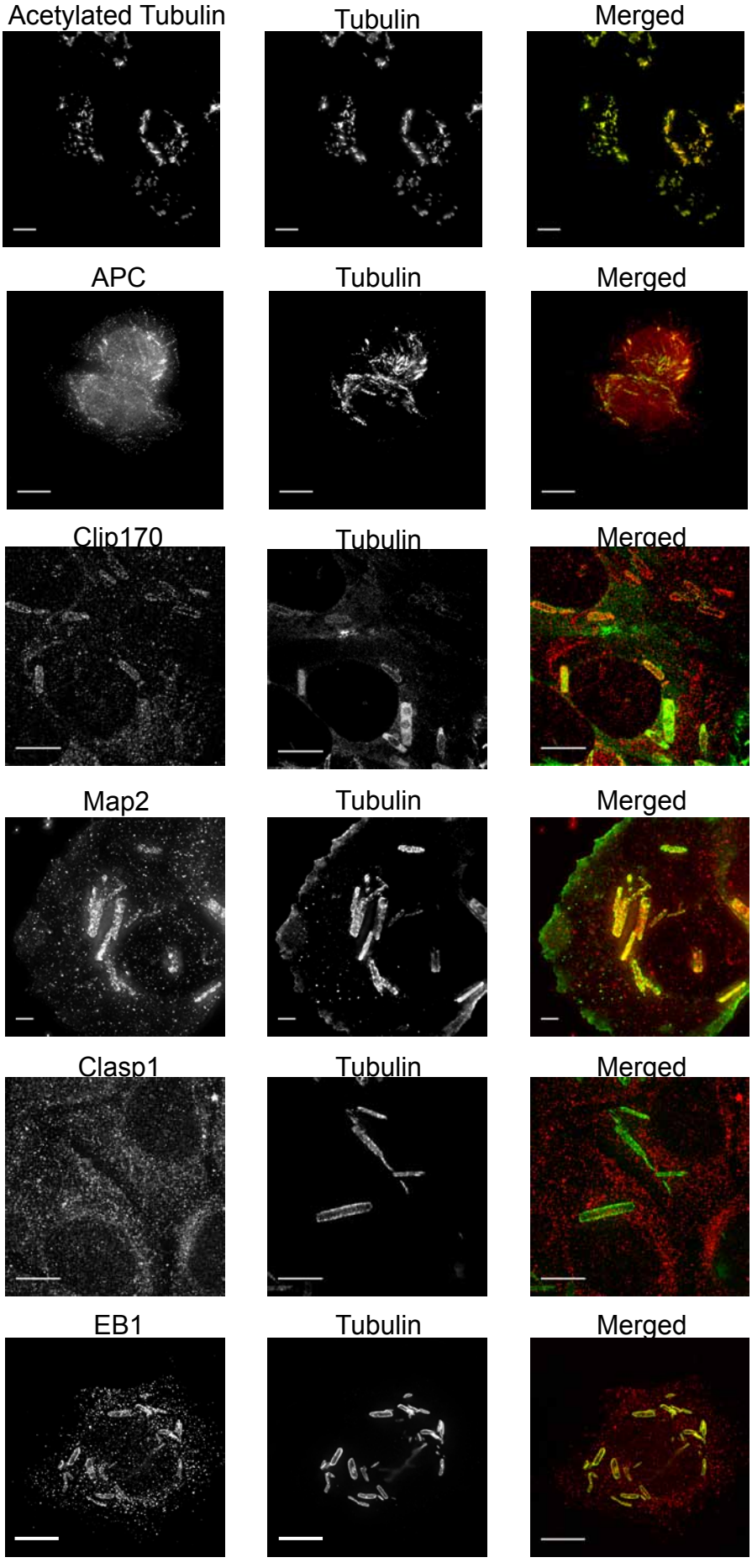
Acetylated Tubulin
Tubulin
Merged
APC
Tubulin
Merged
Clip170
Tubulin
Merged
Map2
Tubulin
Merged
Clasp1
Tubulin
Merged
EB1
Tubulin
Merged

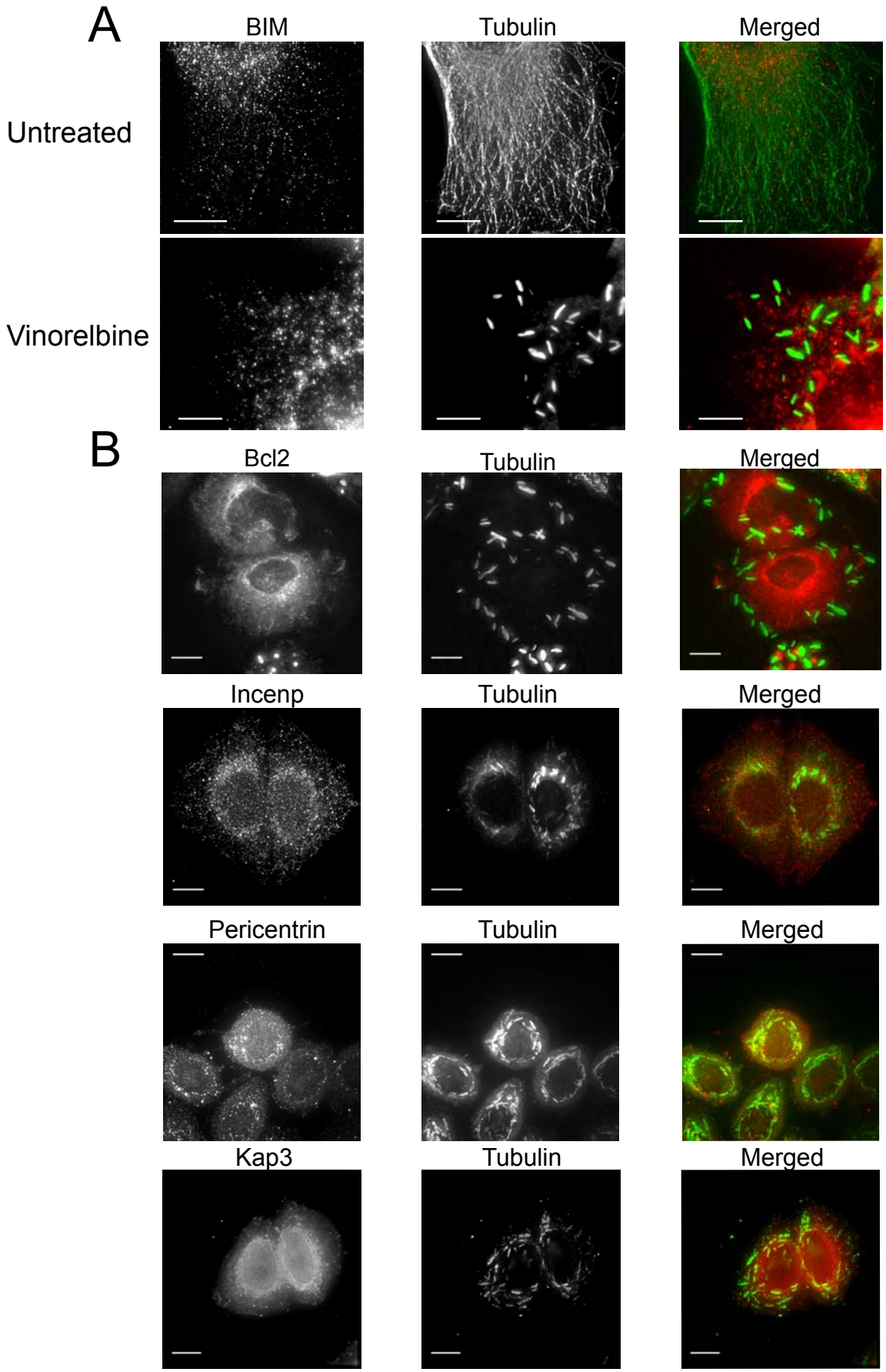
A
BIM
Tubulin
Merged
Untreated
Vinorelbine
B
Bcl2
Tubulin
Merged
Incenp
Tubulin
Merged
Pericentrin
Tubulin
Merged
Kap3
Tubulin
Merged

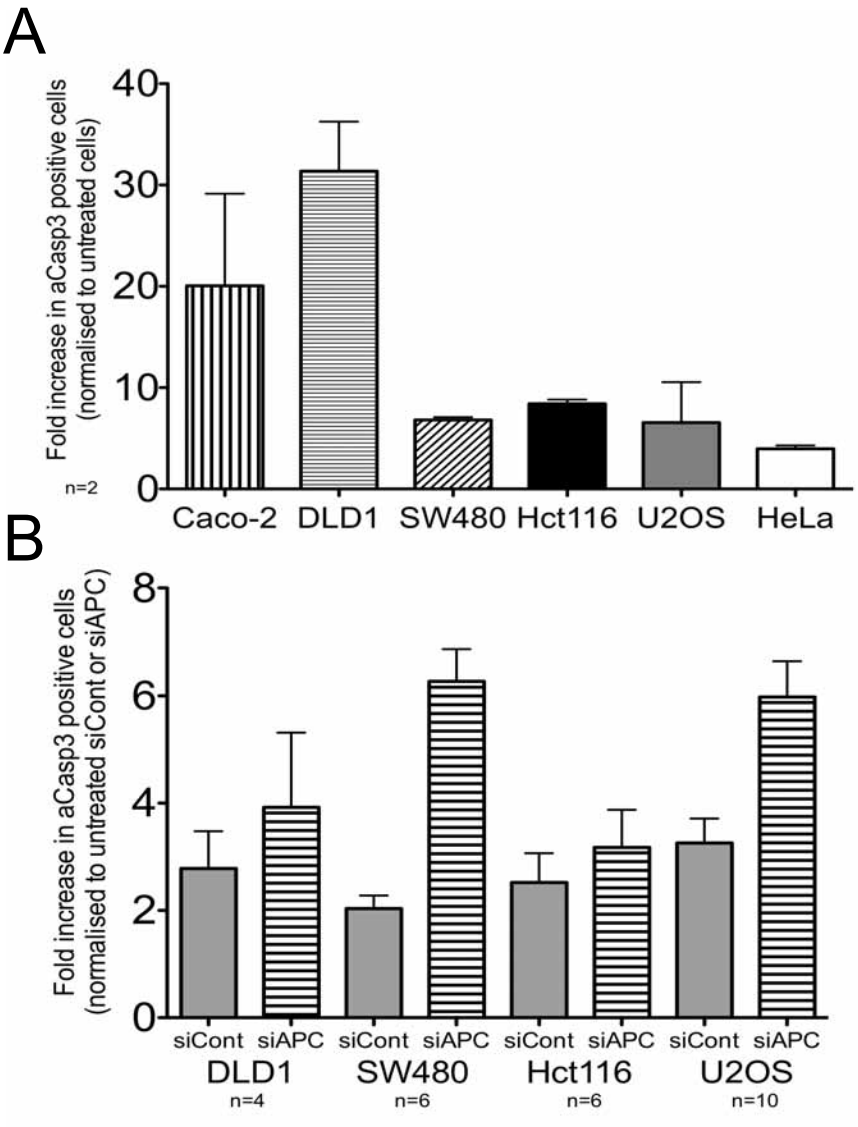
A
Fold increase in aCasp3 positive cells
(normalised to untreated cells)
40
30
20
10
0
n=2
Caco-2
DLD1
SW480
Hct116
U2OS
HeLa
B
Fold increase in aCasp3 positive cells
(normalised to untreated siCont or siAPC)
8
6
4
2
0
siCont
siAPC
DLD1
n=4
SW480
n=6
Hct116
n=6
U2OS
n=10